

Surface Modification of Fly Ash by Thermal Activation: A DR/FTIR Study

Stuti Katara¹, Sakshi Kabra¹, Anita Sharma¹, Renu Hada¹
and Ashu Rani^{1*}

¹Department of Pure and Applied Chemistry, University of Kota, Kota, Rajasthan, India.

Authors' contributions

This work was carried out in collaboration between all authors. Authors SK and AR supervised and designed the study. Author SK (Stuti Katara) performed the experimental and analytical study, wrote the protocol, and wrote the first draft of the manuscript. Authors SK, AS and RH managed the literature searches and helped in analytical study. All authors read and approved the final manuscript.

Research Article

Received 31st March 2013
Accepted 12th July 2013
Published 24th July 2013

ABSTRACT

To acquire a deeper understanding of surface chemistry of fly ash along with thermal activation, the states of mineral phases, water and –OH groups on silica are studied in fly ash at different calcination temperatures by DR/FTIR spectroscopic technique. DR/FTIR spectroscopy allows differentiation of various types of bonds in a material on a molecular level. The spectroscopic results are also supported by XRF, XRD and SEM analysis. Studied fly ash was collected from Jamshedpur Thermal Power Station as an extremely fine ash, formed from the inorganic components of the coal, mainly silica and alumina which remain after combustion of the carbonaceous part of the coal. Distinguish changes were observed in fly ash IR bands regarding absorbed water, -OH group and Si-O-Si group with thermal activation. This investigation reveals that as the temperature increases, the physically adsorbed water begins to remove first, then silanol groups on surface is dehydrated. Increased temperature causes formation of different crystalline phases like quartz, mullite and hematite etc. and increased the crystallinity of the calcined samples.

*Corresponding author: Email: ashu.uok@gmail.com;

Keywords: DR/FTIR; thermal activation; silanol groups; fly ash.

1. INTRODUCTION

The coal fired power plant which consumes pulverized solid fuels composed of combustible organic matter with varying amount of inorganic mineral parts produce large amount of solid waste fly ash. Every year a crude estimation of 600 million tons of fly ash generated worldwide [1] and about 110 million tons only in India [2]. The combustible gasification takes place in coal fired boiler at an operative temperature 1450°C under reducing atmosphere. The mixture of effluent gases is cooled and fly ash gets solidify at temperature from 950°C to 400°C. In the form of spherical particles consisting of SiO₂, Al₂O₃, Fe₂O₃, CaO, MgO and alkali in varying amounts with some unburned activated carbon [3]. As per the ASTM C618-12a guideline [4] the fly ash containing >70% SiO₂, Al₂O₃ and Fe₂O₃ is classified as Class F type fly ash and those consists mainly of silica, alumina and calcium containing SiO₂, Al₂O₃ and Fe₂O₃ minimum upto 50 % are referred to as Class C fly ash. Class F type fly ash is used in agriculture, metal recovery, water and atmospheric pollution control [5] while class C type fly ash is used in cement production [6], steam cured bricks manufacturing [7] etc. Calcination temperature of fly ash before using as source material for synthesis of concrete material and geopolymer etc. is reported to be crucial for the end product [8]. Fly ash has a complex microstructure comprising of mixture of amorphous and crystalline components. The chemical and mineralogical compositions of fly ash vary with coal source as well as calcination temperature [9]. Fly ash also contains different amount of unburned carbon which may reach upto 17% [10] responsible for high ignition loss and undesirable constituents for geopolymerisation and concrete formation. Fly ash is also being used as heterogeneous catalytic support material due to high silica, surface mineralogy, morphology and surface silanol groups [11, 12]. Both the adsorbed water and silanol groups on surface may affect the surface modification process thus play important roles in catalytic application on silica surface. It is difficult to distinguish between the adsorbed moisture and actual surface hydroxyl groups in a form of crystalline water or amorphous silanol (Si-OH) [13]. Literature reports that high temperature calcination forms new crystalline phases on fly ash surface modifying siloxane groups (Si-O-Si) and different forms of silanol groups [8]. Therefore it is of interest to understand the modification of fly ash mineralogy and morphology with thermal activation by using Diffuse Reflectance Fourier Transform Infrared (DR\FTIR) spectroscopic technique, which is one of the advance techniques to illustrate the chemical structure of the bonding materials. The results of the DR\FTIR study are supported by other characterization tools such as X-ray Fluorescence (XRF), X-ray Diffraction (XRD) and Scanning Electron Microscopy (SEM).

2. EXPERIMENTAL DETAILS

2.1 Materials

The coal fly ash (Class F type with SiO₂ and Al₂O₃ > 70%) used in this study was collected from Jamshedpur Thermal Power Station (Jamshedpur, Jharkhand, India). Fly ash (FA) was thermally activated by calcining in muffle furnace at 400, 600, 800 and 1000°C for 3h and abbreviated as TFA-400, TFA-600, TFA-800 and TFA-1000 respectively (TFA –Thermally activated fly ash).

2.2 Sample Preparation and Characterization

DR/FTIR analysis of fly ash samples were carried out by diluting fly ash samples with KBr in 1:20 weight ratio and mixed gently with the help of mortar and pestle, being careful about atmospheric moisture absorption. In this study, FTIR spectra of the materials were recorded using FTIR Tensor 27 Bruker with DR (Diffuse Reflectance) accessory. The spectra were recorded in the range $550 - 4000 \text{ cm}^{-1}$ with a resolution of 4 cm^{-1} . The chemical composition was determined by wavelength dispersive X-ray fluorescence (WD-XRF) model Bruker S8 Tiger. The detailed imaging information about the morphology and surface texture of the sample was provided by SEM (Philips XL30 ESEM TMP). The XRD measurements were carried out using Bruker D8 Advance X-ray diffractometer with monochromatic $\text{CuK}\alpha$ radiation ($\lambda = 1.54056 \text{ \AA}$) in a 2θ range of $5-70^\circ$.

3. RESULTS AND DISCUSSION

The chemical composition of FA and all TFA samples reveals that major components of fly ash are SiO_2 and Al_2O_3 . Some minor components like Fe_2O_3 , CaO , MgO , TiO_2 , Na_2O , K_2O and trace elements around 1.5 wt% are also present in FA and all TFA samples (Table 1). The thermal activation of fly ash removes C, S, moisture and other adsorbed gases. The removal of moisture and co-existing unburned carbon increases with increasing temperature [14]. It can be concluded that all the compounds remained almost constant after thermal treatment, besides a reduction in Na_2O , K_2O and other elements in all TFA samples.

Table 1. Chemical composition of FA and all TFA samples

Sample	SiO_2 (wt%)	Al_2O_3 (wt%)	Fe_2O_3 (wt%)	CaO (wt%)	MgO (wt%)	TiO_2 (wt%)	Na_2O (wt%)	K_2O (wt%)	Other elements (wt%)
FA	62	30	3.0	0.4	0.3	1.4	0.4	0.8	1.7
TFA-400	62.3	30	3.2	0.4	0.3	1.4	0.3	0.5	1.6
TFA-600	62.5	30.1	3.2	0.3	0.3	1.4	0.3	0.3	1.6
TFA-800	62.8	30.3	3.2	0.3	0.2	1.3	0.2	0.2	1.5
TFA-1000	63	30.5	3.2	0.3	0.2	1.3	0.2	0.1	1.2

The FTIR spectra in Fig. 1 shows a broad band between $3400-3000 \text{ cm}^{-1}$, which is attributed to surface $-\text{OH}$ groups of silanol groups ($-\text{Si}-\text{OH}$) and adsorbed water molecules on the surface. The broadness of band indicates the presence of strong hydrogen bonding [11]. The gradual decrement in the intensity and broadness in this band, as shown in Fig. 1 confirms loss of water in all TFA samples during thermal activation. Most of the molecular water gets removed from the sample by heating up to 250°C , while crystalline $-\text{OH}$ remains in the sample till 700°C [15]. A peak around 1607 cm^{-1} (Fig. 1) is attributed to bending mode ($\delta\text{O}-\text{H}$) of water molecule [16] which is shown in all fly ash samples. A broad band ranging from 1070 cm^{-1} to 1170 cm^{-1} due to $\text{Si}-\text{O}-\text{Si}$ asymmetric stretching vibrations [17] of silica is present in FA and all TFA samples. FA shows $\text{Si}-\text{O}-\text{Si}$ asymmetric stretching vibration centered at 1100 cm^{-1} which get shifted towards higher wave number at 1162 cm^{-1} in case of TFA-1000. This high wave number shift is the result of loss of water thus transformation of Q^3 units $[\text{Si}(\text{OH})(\text{SiO}_4)_3]$ to Q^4 units $[\text{Si}(\text{SiO}_4)_4]$ thus decrease in silanol groups ($-\text{Si}-\text{OH}$). This phenomenon shows reverse accordance with the statement that an increase in the hydroxide concentration shifts the position of the maximum absorbance of $\text{Si}-\text{O}$ bands toward lower number, indicating the transformation of Q^4 units $[\text{Si}(\text{SiO}_4)_4]$ to Q^3 units $[\text{Si}(\text{OH})$

(SiO_4)₃] [18]. Peak at 2887 cm^{-1} could be assigned to C-H stretching vibration of organic contaminants which may be introduced during sample handling or some hydrocarbon present in fly ash [17.] This peak shows high intensity in FA while on thermal activation organic contaminants get removed from FA and show low intense peak in all TFA samples as compared to FA. Peaks appeared around 2343 cm^{-1} attributed to ν O-H stretching [19], 2241 cm^{-1} responsible for H-SiO₃ [20], 1984 cm^{-1} due to =Si-H monohydride [21], 1872 cm^{-1} due to calcium carbonate [22] present in FA and all TFA samples (Table 2). Peaks centered at 1521 cm^{-1} [23] and 1681 cm^{-1} [17] are due to $(\text{CO}_3)^{2-}$ stretching vibration show highest intensity in FA, which is reduced on thermal activation in all TFA samples conferring that during thermal activation C and C associated impurities like CO₂ are removed with increased temperature. A peak related to Al-O-Si stretching vibration appears around 600 cm^{-1} [24] and is present in FA and all TFA samples (Table 2) conferring that Si and Al are present in silico aluminate phase not affected by thermal activation [25].

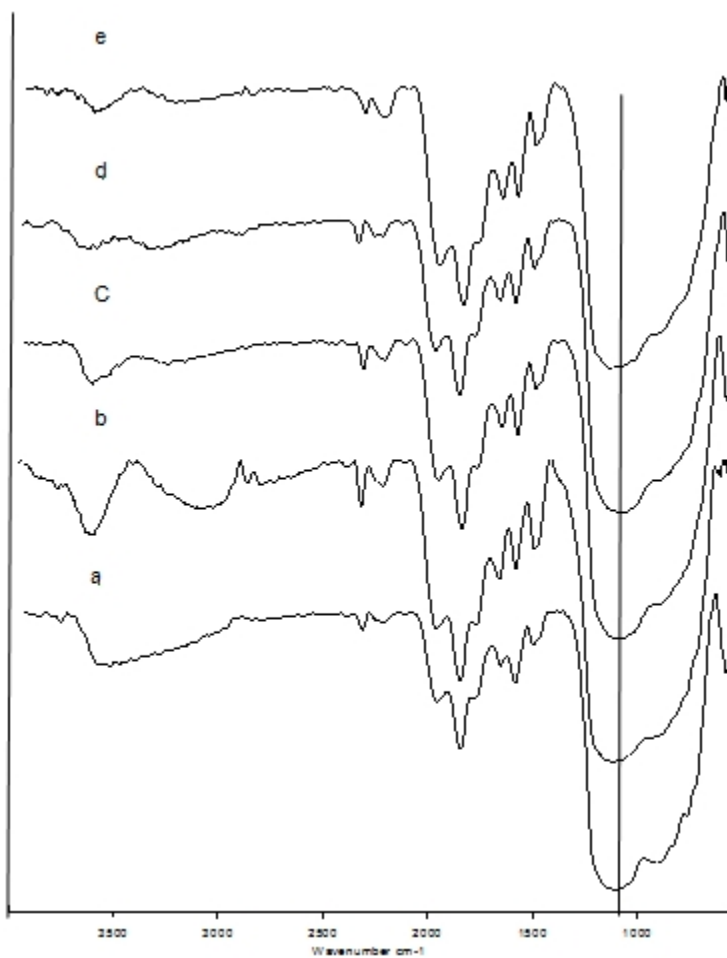


Fig. 1. DR/FTIR spectra of (a) FA (b) TFA-400 (c) TFA-600 (d) TFA-800 (e) TFA-1000
Table 2. Different DR/FTIR observed frequencies of (1.) FA (2.) TFA-400 (3.) TFA-600
(4.) TFA-800 (5.) TFA-1000 and their possible assignments

Assignments	FA	TFA-400	TFA-600	TFA-800	TFA-1000	Reference no.
Si-O-Al stretching vibration	600	611	589	592	603	24
Si-O-Si asymm. Stretching Vibration	1100	1102	1113	1148	1162	17
(CO ₃) ²⁻ —stretching vibration	1521, 1679	1519, 1686	1519, 1680	1519, 1683	1521, 1681	23, 17
H-O-H bending Vibration	1608	1606	1606	1607	1607	16
Calcium Carbonate	1872	1872	1872	1872	1873	22
=Si-H (monohydride)	1984	1984	1986	1984	1987	21
H-SiO ₃	2241	2240	2244	2236	2250	20
v -O-H stretching vibration	2343	2344	2341	2347	2345	19
-C—H stretching vibration	2827	2887	2886	2890	2895	17
-O-H stretching vibration	3553	3096	3276	3327	3260	11

The SEM image (Fig. 2) of FA demonstrates particles of different shapes and sizes, hollow cenospheres, irregularly shaped unburned carbon particles, miner aggregates and agglomerated particles whereas the typical SEM image of TFA-1000 shows different shape and size particles while irregular shaped unburned carbon is not seen. Some fused silica particles are showing which has been formed during thermal activation [11].

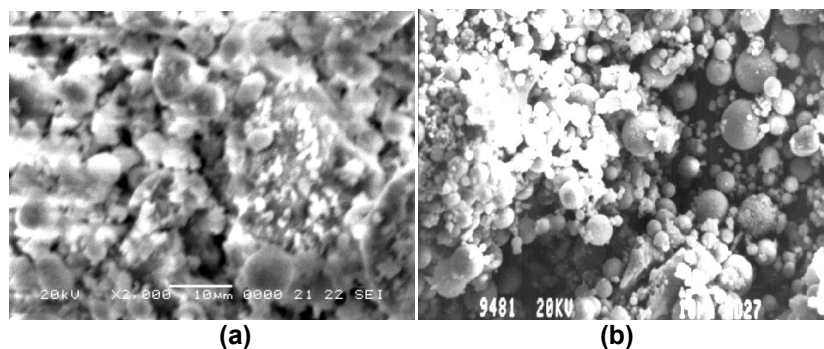


Fig. 2. SEM images of (a) FA (b) TFA-1000

The XRD patterns of FA and TFA-1000 are shown in Fig. 3. In both FA and TFA-1000, peaks at 2θ values of 16.4° , 25.9° and 26.2° show presence of mullite (alumino-silicate)

phases and quartz (silica) exhibits strong peaks at 20.7°, 26.5°, 26.66°, 40.66° and 49.96° of 2θ values [26] while calcite shows peaks at 33.4° of 2θ values [11]. TFA-1000 shows number of crystalline phases like quartz, hematite, mullite, calcite in higher intensities than FA, due to high temperature calcination. With thermal activation magnetite peak tends to disappear while a peak responsible for hematite begins to appear (Table 3) [27].

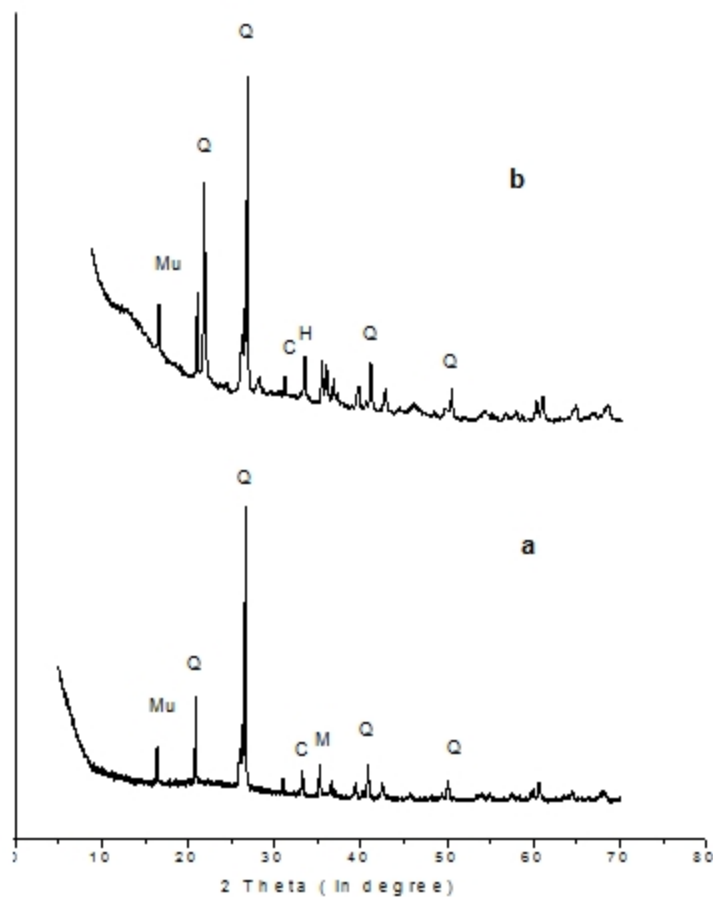


Fig. 3. XRD pattern of (a) FA (b) TFA-1000; (Q- Quartz, Mu- Mullite, M- Magnetite, H- Hematite, C- Calcite)

Table 3. Color and crystalline phases of FA and TFA samples

Sample	Color	Quartz	Magnetite	Hematite	Mullite	Calcite
FA	Grey	√	√	---	√	√
TFA-400	Light grey	√	√	---	√	√
TFA-600	Yellowish brown	√	√	---	√	√
TFA-800	Yellowish brown	√	---	√	√	---
TFA-1000	Reddish brown	√	---	√	√	---

(√ = Present, --- = Absent)

Variation of colors and crystalline phases of FA and TFA calcined at different temperatures is shown in Table 3. Initially fly ash was of grey color due to presence of unburned carbon content with increase in thermal activation temperature grey color of fly ash changes to yellowish brown and then finally red brown possibly due to hematite crystallization [8].

4. CONCLUSION

In each DR/FTIR spectrum broad band ranging from 3000-3400 cm^{-1} is showing a successive decrement in the intensity with increasing thermal activation temperature. It is thus revealed that as the temperature increases, physically adsorbed water is removed first, then silanol groups on surface is dehydrated resulting in transformation of Q^3 units $[\text{Si}(\text{OH})(\text{SiO}_4)_3]$ to Q^4 units $[\text{Si}(\text{SiO}_4)_4]$. Due to thermal activation of fly ash, SiO_2 , Al_2O_3 are increased which is also evidenced by increased intensity of quartz and mullite phases, the magnetite phases are converted into hematite phase at higher temperature. It can be concluded that modification in properties of fly ash with reference to Si-OH, intensity and crystallinity of crystalline phases can be achieved by thermal activation method to generate a solid support material for catalytic applications.

ACKNOWLEDGEMENT

SEM and XRD characterizations were performed at UGC-DAE Consortium for Scientific Research, Indore. The authors are thankful to Dr. D.M. Phase and Er. V.K. Ahiray for SEM-EDX analysis and Dr. Mukul Gupta for XRD analysis. The authors are also thankful to SAIF, Punjab University for their XRF facility. Stuti katara is thankful to University Grants Commission, New Delhi, India for their financial support through Senior Research Fellowship scheme.

COMPETING INTERESTS

Authors have declared that no competing interests exist.

REFERENCES

1. Yao ZT, Xia MS, Ye Y, Zhang L. Synthesis of zeolite Li-ABW from fly ash by fusion method. *J Hazard Mater.* 2009;170(2):639-44. doi:10.1016/j.bbr.2011.03.031.
2. Senapati MR. Fly ash from thermal power plants - waste management and overview. *Curr Sci.* 2011;100(12).
3. Kutchko BG, Kim AG. Fly ash characterization by SEM-EDS. *Fuel.* 2006;85(17):2537-44. doi:10.1016/j.fuel.2006.05.016.
4. American Society for Testing and Materials (ASTM), ASTM C618 – 12a, "Standard specification for coal fly ash and raw or calcined natural pozzolan for use in concrete", Annual book of ASTM standards, Vol.04.02, Philadelphia, Pennsylvania, 1994.
5. Blanco F, Garcia MP, Ayala J. The effect of mechanically and chemically activated fly ashes on mortar properties. *Fuel.* 2006;85(14):2018–26. doi:10.1016/j.fuel.2006.03.031.
6. Sahu S, Majling J. Preparation of sulphoaluminate belite cement from fly ash. *Cem Concr Res.* 1994;24(6):1065-72. doi:10.1016/0008-8846(94)90030-2.
7. Scheetz BE, Earle R. Utilization of fly ash. *Curr Opin Solid State Mater Sci.* 1998;3(5):510-20. doi:10.1016/S1359-0286(98)80017-X.

8. Temuujin J, Riessen AV. Effect of fly ash preliminary calcination on the properties of geopolymer. *J Hazard Mater*. 2009;164:634–39. doi:10.1016/j.jhazmat.2008.08.065.
9. Van Jaarsveld JSG, Van Deventer JSJ, Lukey GC. The characterisation of source materials in fly ash-based geopolymers. *Mater Lett*. 2003;57(7):1272–80. doi: 10.1016/S0167-577X(02)00971-0.
10. Gray ML, Champagne KJ, Soong Y, Killmeyer RP, Maroto-Valer MM, Andresen JM et al. Physical cleaning of high carbon fly ash. *Fuel Process Technol*. 2002;76(1):11–21. doi:10.1016/S0378-3820(02)00006-1.
11. Khatri C, Rani A. Synthesis of a nano-crystalline solid acid catalyst from fly ash and its catalytic performance. *Fuel*. 2008;87(13):2886–92. doi:10.1016/j.fuel.2008.04.011.
12. Jain D, Rani A. MgO enriched coal fly ash as highly active heterogeneous base catalyst for Claisen-Schmidt condensation reaction. *Am Chem Sci J*. 2011;1(2):37-49.
13. Peng L, Qisui W, Xi L, Chaocan Z. Investigation of the states of water and OH groups on the surface of silica. *Colloids and Surfaces A: Physicochem Eng Aspects*. 2009;334:112–15. doi:10.1016/j.colsurfa.2008.10.028.
14. Kordatos K, Gavela S, Ntziouni A, Pistiolas KN, Kyritsi A, Rigopoulou VK. Synthesis of highly siliceous ZSM-5 zeolite using silica from rice husk ash. *Micropor Mesopor Mater*. 2008;115(1-2):189-96. doi:10.1016/S0167-577X(02)00971-0.
15. Richardson IG. The calcium silicate hydrates. *Cem Concr Res*. 2008;38:137–58.
16. Palomo A, Grutzeck MW, Blanco MT. Alkali-activated fly ashes a cement for the future. *Cem Concr Res*. 1999;29:1323-29.
17. Saikia BJ, Parthasarthy G, Sarmah NC, Baruah GD. Fourier-transform infrared spectroscopic characterization of naturally occurring glassy fulgurites. *Bull Mater Sci*. 2008;31(2):155–58.
18. Morten ES, Camilla S, Li Z, Sogaard EG. Xps and Ft-Ir Investigation of Silicate Polymers. *J Mater Sci*. 2009;44:2079–88. doi:10.1007/s10853-009-3270-9.
19. Zaki MI, Knozinger H, Tese B, Mekhemer GAH. Influence of phosphonation and phosphation on surface acid–base and morphological properties of CaO as investigated by in situ FTIR spectroscopy and electron microscopy. *J colloid Interface Sci*. 2006;303(1):9-17. doi: 10.1016/j.jcis.2006.07.011.
20. Sun XH, Wang SD, Wong NB, Ma DDD, Lee ST, Teo BK. FTIR spectroscopic studies of the stabilities and reactivities of hydrogen-terminated surfaces of silicon nanowires. *Inorg Chem*. 2003;42(7):2398-404. doi:10.1021/ic020723e.
21. Blanco F, Garcia MP, Ayala J. Variation in fly ash properties with milling and acid leaching. *Fuel*. 2005;84(1):89-96. doi:10.1016/j.fuel.2004.05.010.
22. Jacox EM. Vibrational and Electronic Energy Levels of Polyatomic Transient Molecules Supplement B. *J Phys Chem Ref Data*. 2003;32(1). doi: 10.1063/1.1497629.
23. Handa H, Baba T, Sugisawa H, Ono Y. Highly efficient self-condensation of benzaldehyde to benzyl benzoate over KF-loaded alumina. *J Mol Catal A Chem*. 1998;134(1):171-77. doi:10.1016/S1381-1169(98)00033-8.
24. Frances IH, Denisse VA, Meghan EG. High temperature aerogels in the Al₂O₃-SiO₂ system. Presented at the American chemical society 236th national meeting Philadelphia, Pa, August 20, 2008. Accessed 24 May 2013. Available: <http://usrp.usra.edu/technicalPapers/glenn/arrandaAug08.pdf>.
25. Temuujin J, Okada K, Kenneth JDM. Preparation and properties of potassium aluminosilicate prepared from the waste solution of selectively leached calcined kaolinite. *Appl Clay Sci*. 2002;21:125–31. doi:10.1016/S0169-1317(01)00082-5.
26. Sharma A, Srivastava K, Devra V, Rani A. Modification in Properties of Fly Ash through Mechanical and Chemical Activation. *Am Chem Sci J*. 2012;2(4):177-87.

27. Fox JM. Changes in fly ash with thermal treatment. Presented in 2005 World of Coal Ash (WOCA), April 11-15,2005, Lexington, Kentucky, USA. Accessed 24 May 2013. Available: <http://www.flyash.info/2005/132fox.pdf>.

© 2013 Katara et al.; This is an Open Access article distributed under the terms of the Creative Commons Attribution License (<http://creativecommons.org/licenses/by/3.0>), which permits unrestricted use, distribution, and reproduction in any medium, provided the original work is properly cited.

Peer-review history:

The peer review history for this paper can be accessed here:
<http://www.sciencedomain.org/review-history.php?iid=245&id=7&aid=1733>